

Cohesive properties of noble metals by van der Waals-corrected Density Functional Theory

Alberto Ambrosetti and Pier Luigi Silvestrelli

Dipartimento di Fisica e Astronomia, Università di Padova,

via Marzolo 8, I-35131, Padova, Italy,

and DEMOCRITOS National Simulation Center,

of the Italian Istituto Officina dei Materiali (IOM) of the

Italian National Research Council (CNR), Trieste, Italy

Abstract

The cohesive energy, equilibrium lattice constant, and bulk modulus of noble metals are computed by different van der Waals-corrected Density Functional Theory methods, including vdW-DF, vdW-DF2, vdW-DF-cx, rVV10 and PBE-D. Two specifically-designed methods are also developed in order to effectively include dynamical screening effects: the DFT/vdW-WF2p method, based on the generation of Maximally Localized Wannier Functions, and the RPAp scheme (in two variants), based on a single-oscillator model of the localized electron response. Comparison with results obtained without explicit inclusion of van der Waals effects, such as with the LDA, PBE, PBEsol, or the hybrid PBE0 functional, elucidates the importance of a suitable description of screened van der Waals interactions even in the case of strong metal bonding. Many-body effects are also quantitatively evaluated within the RPAp approach.

I. INTRODUCTION

van der Waals (vdW) interactions are ubiquitous in nature and can be of importance even in densely packed systems, characterized by strong ionic, covalent, or metallic bonds, where these types of interactions are commonly assumed to be negligible.^{1,2}

In particular, the effect of vdW forces in noble metals has been investigated a long time ago by Rehr and Zaremba³ who adopted a simplified model in which the ions are regarded as nonoverlapping (with the core electrons which are relatively well localized) and immersed in a uniform electron gas made by the conduction electrons. Therefore, in spite of the hybridization between bands, the optical properties are reasonably well described by first separating the electrons into polarizable core states embedded in a quasifree-electron gas.⁴ This corresponds⁴ to regarding the d electrons as localized atomic orbitals in the spirit of the tight-binding approximation, while treating the s electrons with nearly-free-electron theory. By taking into account the conduction-electron screening of the ion-ion interactions and using effective ionic polarizabilities derived from the measured optical constants, the vdW contribution to the cohesive energy per atom was found³ to be 0.21, 0.42, and 0.63 eV for Cu, Ag, and Au, respectively in the equilibrium face-centered cubic geometry (FCC, see Fig. 1). These values should be compared to the total cohesive energies in these metals, which are 3.50, 2.96, and 3.78 eV, respectively. On going from Cu to Ag to Au, the increasing magnitude of the polarizability reflects the increasingly larger low-frequency oscillator strengths, with a significant part of the low-frequency oscillator strengths that is attributable to d -electron transitions.³ Interestingly, Rehr and Zaremba obtained an expression for the dipole-dipole contribution to the polarization force which is analogous to the usual expression for the vdW interaction between atoms in a molecular crystal.⁴ The presence of the electron gas gives rise to a dynamically screened interaction between the ions described by the dielectric function of the electron gas which is approximated by the random-phase approximation (RPA) expression evaluated for the values of the r_s parameters corresponding to the “free-electron” densities of the noble metals. In the simplest model one assumes that the core fluctuations are dominated by a single excited state leading to an approximated formula for the screened vdW interactions in a polarizable metal.⁴ This approximation is certainly crude for a noble metal since excitations to a continuum in the range 5-50 eV are important, but the result demonstrates an essential qualitative point, namely that if

the dielectric constant does not show substantial momentum dependence, dispersion forces approximately keep their usual asymptotic form even in the presence of dynamic screening by an electron gas.⁴ As expected, the screening is most effective for frequencies smaller than the plasma frequency. Contributions to the polarization forces due to higher-order terms than the dipole-dipole one are estimated to increase the vdW correction by roughly 20%.³ The above description applies equally to any simple metal which has a highly polarizable core, but whose core electrons may be well separated from the $s - p$ band.⁴

From a theoretical point of view, it is well accepted that Density Functional Theory (DFT), which represents the most popular and widely adopted ab initio approach for condensed-matter calculations, fail to capture vdW forces, at least within the standard implementations based on the Local Density Approximation (LDA) or the Generalized Gradient Approximation (GGA), which are still the most used for the calculations of structural and electronic properties of solids. In the last years several practical methods have been proposed to make DFT calculations able to accurately describe vdW effects at a reasonable computational cost (see, for instance, refs. 5–7). We have developed a family of such methods, all based on the generation of the Maximally Localized Wannier Functions (MLWFs),⁸ successfully applied to a variety of systems, including small molecules, water clusters, graphite and graphene, water layers interacting with graphite, interfacial water on semiconducting substrates, hydrogenated carbon nanotubes, molecular solids, and the interaction of rare gases, small molecules, and graphene with metal surfaces.^{9–22} Of a particular value is the possibility of dealing with metals; in fact insulators could be somehow treated even using atom-based semiempirical approaches where an approximately derived R^{-6} term, multiplied by a suitable short-range damping function, is explicitly introduced. Instead, in our methods the atom-based point of view assumed in standard semiempirical approaches is replaced by an electron-based point of view, so that the schemes are also naturally applicable to systems, such as metals and semimetals, which cannot be described in terms of assemblies of atoms only weakly perturbed with respect to their isolated configuration. Besides electron-based models, effective approaches may also be designed in such a way to separate local and non-local polarizability components. Although the polarizability disentanglement is a non-trivial procedure which requires detailed information on the electronic structure of the system, the introduction of a suitably parameterized atom-based model Hamiltonian can thus provide an alternative pathway to the computation of vdW interactions.²³ We re-

mark that in the case of vdW-corrected DFT schemes applied to metallic systems a proper inclusion of screening effects is essential.^{19,24} We also stress that cross-validation between independent vdW methods not only permits a more rigorous accuracy benchmarking, but also provides better insight into the relevant physical ingredients of the theory.

In order to unravel the role of long-range correlation and screening effects, we assess here the performance of different vdW-corrected Density Functional Theory methods applied to the description of cohesive properties of bulk noble metals. In particular, to capture complex dynamical screening effects, we develop a specific version (see below) of our DFT/vdW-WF2 approach,¹⁹ and the RPAp scheme, based on a single-oscillator model of the localized electron response (see below). Moreover, we consider the dispersion corrected PBE (PBE-D²⁵), vdW-DF,^{26,27} vdW-DF2,²⁸ vdW-DF-cx,^{29,30} rVV10³¹ methods, the TPSS³² and PBE0³³ functionals, and the simpler Local Density Approximation (LDA) and semilocal GGA (in the PBE³⁴ and PBEsol³⁵ flavors) approaches. PBEsol³⁵ is a simple revision of PBE to improve the description of solids and surfaces. In the PBE-D scheme DFT calculations at the PBE level are corrected by adding empirical C_6/R^6 potentials with parameters derived from accurate quantum chemistry calculations for atoms, while in other methods, such as vdW-DF, vdW-DF2, vdW-DF-cx, and rVV10, vdW effects are included by introducing DFT nonlocal correlation functionals. In particular, vdW-DF^{26,27} denotes the first version of the Rutgers-Chalmers functional, vdW-DF2²⁸ the second version which updates both the exchange and correlation functional to improve the description of bonding among small molecules, vdW-DF-cx^{29,30} one of the most recent versions based on a different exchange functional, and rVV10³¹ is the revised, more efficient version of the original VV10 scheme³⁶ which relies on the optimization of two parameters using a reference database. Finally, TPSS³² is a meta-GGA functional whose mathematical form is based on the PBE functional,³⁷ while PBE0^{33,38} denotes a hybrid functional which combines PBE with a given fraction of exact exchange.

II. SCREENED VDW METHODS

We propose and apply here two independent theoretical methodologies for the computation of screened vdW energy contributions in bulk metallic systems. Both approaches are based on a distinction between localized electrons contributing to the local polarizability,

and delocalized states, which –in analogy to the homogeneous electron gas– introduce a dynamical screening of the Coulomb interaction, as outlined in Fig. 2. The screening is effectively described through a frequency-dependent dielectric function, which we approximate through a single-pole expression (see refs. 3,4) as

$$\epsilon(iu) = 1 + \frac{\omega_p^2}{u^2}, \quad (1)$$

where ω_p is the plasma frequency of the *electron gas*. Then, by exploiting the adiabatic connection fluctuation-dissipation (ACFD) formula,³⁹ where use is made of the *dressed* Coulomb interaction, by integration over the frequency one obtains the dynamically screened vdW energy.

Different approaches, instead, are followed for describing the polarizability of localized electrons. In the first method (DFT/vdW-WF2p – where “p” indicates the introduction of plasmon pole screening) a MLWF partitioning of the electronic charge is introduced, which allows a transparent and straightforward separation between localized and delocalized states. The second method (denoted as RPAp), instead is based on a single-oscillator description of the localized electron response, inspired by the recent MBD method,^{39,40} and permits to compute many-body dispersion effects within the RPA.

A. DFT/vdW-WF2p

Our DFT/vdW-WF2 method (see additional details in refs. 18,19) relies on the well known London’s expression⁴¹ where two interacting atoms, A and B , are approximated by coupled harmonic oscillators and the vdW energy is taken to be the change of the zero-point energy of the coupled oscillations as the atoms approach; if only a single excitation frequency is associated to each atom, ω_A , ω_B , then

$$E_{vdW}^{London} = -\frac{C_6^{AB}}{R_{AB}^6} = -\frac{3e^4}{2m^2} \frac{Z_A Z_B}{\omega_A \omega_B (\omega_A + \omega_B)} \frac{1}{R_{AB}^6} \quad (2)$$

where $Z_{A,B}$ is the total charge of A and B , and R_{AB} is the distance between the two atoms (e and m are the electronic charge and mass).

Now, adopting a simple classical theory of the atomic polarizability, the polarizability of an electronic shell of charge eZ_i and mass mZ_i , tied to a heavy undeformable ion can be written as

$$\alpha_i \simeq \frac{Z_i e^2}{m \omega_i^2}. \quad (3)$$

Then, given the direct relation between polarizability and atomic volume,⁴² we assume that $\alpha_i = \gamma S_i^3$, where γ is a proportionality constant, so that α_i is expressed in terms of the MLWF spread, S_i . Recasting eq. (2) in terms of the quantities defined above, one obtains an explicit expression for the C_6^{ij} vdW coefficient relative to the vdW interaction between the i -th and the j -th electronic orbitals belonging to different fragments:

$$C_6^{ij} = \frac{3}{2} \frac{\sqrt{Z_i Z_j} S_i^3 S_j^3 \gamma^{3/2}}{(\sqrt{Z_j} S_i^{3/2} + \sqrt{Z_i} S_j^{3/2})}. \quad (4)$$

In previous applications^{18,19} the proportionality constant γ was set up by imposing that the exact value for the H atom polarizability ($\alpha_H = 4.5$ a.u.) is obtained. Here, a more convenient choice (see also below) for γ is to impose that, by summing the contributions to the polarizability coming from the d -like MLWFs describing the core ions, one reproduces the experimental effective ionic polarizabilities derived from the measured optical constants:³ $\alpha_{ion} = \sum_i \alpha_i = \sum_i \gamma S_i^3$.

In order to achieve a better accuracy, one must properly deal with *intrafragment* MLWF charge overlap. This overlap affects the effective orbital volume, the polarizability, and the excitation frequency (see eq. (3)), thus leading to a quantitative effect on the value of the C_6 coefficients. We take into account the effective change in volume due to intrafragment MLWF overlap by introducing a suitable reduction factor ξ obtained by interpolating between the limiting cases of fully overlapping and non-overlapping MLWFs (see ref. 18). We therefore arrive at the following expression for the C_6 coefficient:

$$C_6^{ij} = \frac{3}{2} \frac{\sqrt{Z_i Z_j} \xi_i S_i^3 \xi_j S_j^3 \gamma^{3/2}}{(\sqrt{Z_j \xi_i} S_i^{3/2} + \sqrt{Z_i \xi_j} S_j^{3/2})}, \quad (5)$$

where $\xi_{i,j}$ represents the ratio between the effective and the free volume associated to the i -th and j -th MLWF.

Finally, the vdW interaction energy is computed as:

$$E_{vdW} = - \sum_{i < j} f(R_{ij}) \frac{C_6^{ij}}{R_{ij}^6}, \quad (6)$$

where $f(R_{ij})$ is a short-range damping function which maintains the same basic functional form adopted in previous applications^{18,19} but it is slightly modified following the prescription proposed by Tkatchenko and Scheffler⁴³ and is defined as :

$$f(R_{ij}) = \frac{1}{1 + e^{-a(R_{ij}/R_s - 1)}}. \quad (7)$$

We remark that this short-range damping function is introduced not only to avoid the unphysical divergence of the vdW correction at small fragment separations, but also to eliminate double countings of correlation effects, by considering that standard DFT approaches properly describe short-range correlations.

The parameter R_s is proportional to the sum of the vdW radii: $R_s = s(S_i + S_j)$, with $s = 0.94$ (that is a value optimized for the underlying PBE functional⁴³) and, following Grimme *et al.*,⁴⁴ $a \simeq 20$; note that the results are only mildly dependent on the particular value of this parameter, at least within a reasonable range around the $a = 20$ value. Although this damping function introduces a certain degree of empiricism in the method, we stress that a is the only ad-hoc parameter present in our approach, while all the others are only determined by the basic information given by the MLWFs, namely from first principles calculations. In practice, since we focus on bulk noble metals with interatomic distances corresponding to lattice constants close to the experimental values, the damping function defined above is effective (that is its value is significantly smaller than 1) only for bulk Cu, since in this case the average sum of the spreads of 2 MLWFs belonging to adjacent Cu atoms (2.55 Å) is very close to the interatomic distance (2.55 Å, at the experimental lattice constant), while this is not the case for Ag and Au which are characterized by larger nearest-neighbor distances (the literature reference data for the experimental lattice constants of Cu, Ag, and Au are 3.61, 4.09, and 4.08 Å, respectively).

To get an appropriate inclusion of metal screening effects we adopt the approximated formula⁴ for the screened vdW interactions in a polarizable metal (see above) based on the plasma frequency, which consists in multiplying the C_6^{ij}/R_{ij}^6 contribution in eq. (6) by the reduction factor: $(w_{ij}/(w_{ij} + w_p))^3$, where w_{ij} denotes the average excitation frequency attributed to the i -th and j -th MLWFs, $w_{ij} = (w_i + w_j)/2$, with $w_i = \sqrt{Z_i/(\gamma\xi_i S_i^3)}$, and w_p is the plasma frequency, which can be directly related to the metal r_s parameter: $w_p \propto r_s^{-3/2}$.

Therefore, in summary, our vdW-WF2 scheme specifically developed for dealing with noble-metal bulk systems, hereafter referred to as vdW-WF2p, differs from the previous

versions essentially in: (i) a different choice of the γ parameter to reproduce ionic polarizabilities, (ii) a modified damping function, and (iii) a different implementation of the metal screening correction (based on the plasma frequency), that in previous applications was only aimed at describing adsorption processes on metal substrates.

B. RPAp

Analogously to DFT/vdW-WF, RPAp is based on an effective model, where the response of strongly bound electrons is described in terms of localized atomic polarizabilities, interacting through a uniform medium described by the dielectric function of eq.(1).

The localized ionic polarizabilities are mapped into the response of single quantum Drude oscillators, coupled via dipole-dipole interaction. The resulting effective Hamiltonian is written as^{39,40}

$$H = -\frac{1}{2} \sum_{p=1}^N \nabla_{\boldsymbol{\mu}_p}^2 + \frac{1}{2} \sum_{p=1}^N \omega_p^2 \boldsymbol{\mu}_p^2 + \sum_{p>q}^N \omega_p \omega_q \sqrt{\alpha_p^0 \alpha_q^0} \boldsymbol{\mu}_p \boldsymbol{\mathfrak{T}}_{pq} \boldsymbol{\mu}_q, \quad (8)$$

where each atom p is characterized by a static dipole polarizability, α_p^0 , and a characteristic oscillator frequency, ω_p , while $\boldsymbol{\mu}_p$ represents the charge displacement of atom p from its equilibrium position, \mathbf{R}_p . The dipole interaction tensor is defined as $\boldsymbol{\mathfrak{T}}_{pq} = \nabla_{\mathbf{R}_p} \otimes \nabla_{\mathbf{R}_q} v(R_{pq})$, where $v(R_{pq})$ is the (frequency dependent) dynamically screened Coulomb interaction acting between atoms p and q . As in DFT/vdW-WF2p, a simple, parameter-free short range damping is introduced, following ref. 39.

While in DFT/vdW-WF2p the charge partitioning is naturally accomplished through the use of the MLWFs, a different approach is adopted in RPAp: following ref. 3, we make use of the ionic polarizability extracted from optical data by subtracting the *free electron* contribution. The ionic polarizability is then fitted through a Lorentzian expression, corresponding to the response of a single Drude oscillator:

$$\alpha_{ion}(iu) = \frac{\alpha_0}{1 + u^2/\omega_0^2}. \quad (9)$$

The static polarizability α_0 is set to the reference value of ref. 3, while two alternative fitting schemes are proposed in order to determine the optimal oscillator frequency ω_0 .

As a first approach (RPAp1), ω_0 is chosen in such a way to reproduce the dipole-dipole screened dispersion energies reported in ref. 3 at second perturbative order. In order to check

the accuracy of the single Drude oscillator approximation, a second approach (RPAp2) is also adopted, namely, ω_0 is straightforwardly obtained by fitting the frequency-dependent polarizability curves of ref. 3 through eq.(9).

Once the effective Hamiltonian is parameterized (see data in Table I), the screened vdW energy is computed at the RPA level via the ACFD formula:³⁹

$$E_{\text{RPAp}} = \frac{1}{2\pi} \int_0^\infty du \text{Tr}[\ln(1 - AT)], \quad (10)$$

where A is a diagonal matrix defined as $A_{ij} = -\alpha_{ion}(iu)\delta_{ij}$. We stress that, at variance with refs. 39,40, explicit integration over frequency u is necessary here, due to the presence of the dynamically screened Coulomb interaction.

C. Computational details

We here apply our specific version of the DFT/vdW-WF2 method described above (vdW-WF2p) and the RPAp scheme in the two variants (RPAp1 and RPAp2) to compute the basic cohesive properties, namely cohesive energy, equilibrium lattice constant, and bulk modulus of noble metals Cu, Ag, and Au. All calculations have been performed with the Quantum-ESPRESSO ab initio package⁴⁵ and the MLWFs have been generated as a post-processing calculation using the WanT package.⁴⁶ We consider a periodically-repeated simulation cell (corresponding to the FCC crystal structure appropriate for noble metals) containing a single metal atom. Electron-ion interactions were described using ultrasoft pseudopotentials (norm-conserving for TPSS calculations) by explicitly including 11 valence electrons per metal atom. As done in previous studies⁴⁷ we adopted a $16 \times 16 \times 16$ k -point sampling of the Brillouin Zone.

To obtain the cohesive energy per atom, simulations were also performed by considering isolated metal atoms contained in a large supercell, so that to make spurious inter-atomic interactions negligible. To this aim spin-polarized calculations were carried out since the relative spin polarization vanishes in solids around equilibrium, but not in their free atoms,⁴⁸ given the presence of an odd number of valence electrons. Using the DFT/vdW-WF2p approach the vdW correction to the cohesive energy per atom is obtained (similarly to what done to estimate the dipole-dipole interaction in ref. 3) by summing one half of the contribution coming from the interaction of the MLWFs reference supercell with

the periodically-repeated MLWFs (considering the periodic FCC structure), the sum being rapidly convergent.⁴⁹ Calculations were carried out by varying the lattice constant from about -3% to $+3\%$ with respect to the experimental equilibrium value; then the cohesive-energy curve is fitted using the Murnaghan equation⁵⁰ to estimate the precise equilibrium values.

For our DFT/vdW-WF2p calculations we chose the PBE³⁴ reference DFT functional, which is probably the most popular GGA functional, provides excellent results in many cases, and is the standard functional for solid-state calculations. As often done in recent studies (see, for instance, ref. 51), the PBE functional was also adopted to generate pseudopotentials used in all the other vdW-corrected schemes we applied, although, in principle one could generate pseudopotentials consistent with the specific functionals (for instance belonging to the vdW-DF family). Extensive tests on many systems showed that this approach is reasonable since the underlying approximation is small and this avoids using pseudopotential that are not well tested as the PBE ones.

Since we are investigating bulk interatomic distances close to the experimental equilibrium values, in order to make the calculations more efficient, for each system, the MLWFs were generated only at the experimental lattice constants and using a $8 \times 8 \times 8$ k -point sampling of the Brillouin Zone: in fact optimizing the MLWF spread with several k points typically leads to quite slow convergence process; we have tested that these approximations do not introduce sizeable errors.

As discussed in the Introduction section, in bulk noble metals one can safely consider^{3,4} the d electrons as localized orbitals, while the s electrons can be described with nearly-free-electron theory. Therefore, in our DFT/vdW-WF2p approach, the vdW-correction was implemented by considering the contribution from the MLWFs generated by the optimizing process including only the narrowest energy window containing 5 bands (the d -like ones), which represents a well-defined criterium to minimize mixing with other states.⁵²

Regarding the RPAp method, due to the slow convergence of many body effects with respect to the system size, all calculations are performed in real space, adopting periodic boundary conditions and making use of an extended cubic supercell containing 864 atoms. Clearly, both the frequency integration and the relatively large size of the adopted supercell imply a non-negligible computational overload with respect to DFT/vdW-WF2p. The higher computational cost, however, is justified by the possibility to estimate non-trivial energy

contributions beyond finite-order perturbative approaches.

III. RESULTS AND DISCUSSION

In Tables II-IV we report the equilibrium cohesive energy, lattice constant, and bulk modulus of bulk Cu, Ag, and Au, computed by using our DFT/vdW-WF2p and RPAp schemes, and the other different methods discussed above. The *cohesive energy*, E_c , is defined as

$$E_c = E_{free} - E \quad (11)$$

where E_{free} is the total energy of the isolated free metal atom (contained in a large supercell, see above) and E is instead the total energy (per atom) of the bulk metal.

In order to get a more reliable comparison with experimental results, the zero-point phonon and finite-temperature effects should be properly taken into account,^{37,48} since experimental quantities are often measured at room temperature so that they are not directly comparable with the results of ground-state electronic structure calculations performed at 0 K. In particular, the zero-point phonon effects correspond to a zero-point anharmonic expansion which tends to make the optimal lattice-constant larger. For instance, the uncorrected experimental results are closer to PBE than LDA, while the experimental values corrected by zero-point phonon effects are smaller and thus closer to LDA values.⁴⁸ Moreover, temperature and phonon effects can modify the bulk modulus up to 5%-8% for metals so that the corrected experimental bulk moduli are stiffer on average. Finally, also the experimental cohesive energies must be corrected by the zero-point vibration energy calculated from the Debye temperature.⁴⁸ In Table V we report the mean relative error (MRE), the mean absolute relative error (MARE) of the cohesive energy, lattice constant and bulk modulus, and the MARE value averaged over the 3 different quantities considered (AMARE); the MREs and the AMARE are also plotted in Fig. 3. As can be seen, the equilibrium lattice constant is reasonably reproduced by all the methods, while the same is not true for the cohesive energy and the bulk modulus which are much more sensitive to the chosen approach.

First considering the LDA and (GGA) PBE functionals, one can see that both give errors in the estimated cohesive energy and bulk modulus of comparable magnitude (AMARE=12.3% and 11.3%, respectively) though of opposite sign (see Fig. 3), as already noticed in the literature (see, for instance, refs. 37,48): LDA systematically overestimates cohesive en-

ergy and bulk modulus while PBE underestimates these quantities. Moreover LDA slightly underestimates the lattice constant while PBE (more significantly) overestimates it. Clearly, neither LDA nor PBE turns out to be adequate for an accurate description of bulk noble metals. The (GGA) PBEsol functional,³⁵ characterized by a modification of the exchange contribution of the original PBE to better describe solids, evidently improves considerably the performances with respect to PBE (AMARE= 6.4%), although a tendency to overestimate particularly the cohesive energy and the bulk modulus can be observed, again in line with previous findings.⁴⁸ Notice that LDA, and the (GGA) PBE and PBEsol functionals by construction cannot properly describe vdW effects. Since the PBE functional reduces to LDA for homogeneous electron densities, in principle the metallic electrons should be already accurately described within PBE. However, while this is probably true for simple metals like Na (PBE underestimates the cohesive energy by less than 5%, see ref. 48), the application to noble metals, characterized by a large fraction (10/11) of relatively localized *d*-like electrons, shows that PBE misses a significant portion of the interaction leading to an underestimate of the cohesive energy and bulk modulus and an overestimate of the lattice constant. We can classify this neglected part of the interaction as “vdW interaction”, although, vdW-corrected PBE calculations often tend to overbind because of an overestimate of the long-range part of the exchange contribution.^{11,14,26,47}

The PBE-D functional, including vdW correction by a semiempirical approach,²⁵ is only marginally superior (AMARE= 9.3%) to LDA and PBE, but worse than PBEsol; in fact, it overestimates the cohesive energy (as LDA) and underestimates the bulk modulus (as PBE).

In principle, seamless vdW-corrected DFT methods, based on genuine nonlocal functionals, should perform better than PBE-D, particularly for metals, where an empirical, atom-based vdW correction is expected to be not adequate. However, as can be seen from Tables II-IV and Fig. 3, different schemes, belonging to this class of approaches, perform quite differently for bulk noble metals. In fact, rVV10 (AMARE= 10.5%) is worse than PBE-D and does not even significantly improve over PBE, by clearly overestimating the lattice constants and underestimating the cohesive energy and (above all) the bulk modulus. The situation is even worse for vdW-DF and vdW-DF2 (AMARE= 20.8% and 19.6%, respectively), where the errors involved in the estimate of the equilibrium lattice constants (too large) and cohesive energies (too small) are particularly evident. Instead, the vdW-DF-cx variant^{29,30} of the vdW-DF family clearly represents a remarkable improvement for

describing the basic properties of the noble metals, with AMARE= 3.5%, the agreement with experimental data being particularly striking for Ag.

In order to assess the relevance of a proper description of dynamical screening effects in noble metals we now turn to the specifically developed approaches presented in Section II. Remarkably, our DFT/vdW-WF2p, RPAp1, and RPAp2 methods exhibit performances similar to vdW-DF-cx (AMARE= 4.7%, 4.3%, and 4.9%, respectively), again giving excellent results for Ag and improving over PBEsol. By comparison of the DFT/vdW-WF2p data with the same quantities evaluated without taking the conduction-electron screening into account (for brevity this method is denoted as DFT/vdW-WF2, see Tables II-IV and Fig. 3), it is clear that the cohesive energy is substantially overestimated by the latter approach, which also predicts a too large bulk modulus and underestimates the equilibrium lattice constant (AMARE= 27.2%). This is clearly due to the fact that the vdW-correction of eq. (6) is too large if the reduction factor $(w_{ij}/(w_{ij} + w_p))^3$ is not included, as confirmed by Table VI, where the vdW contribution to the cohesive energy, E_{vdW} , defined as the difference between the equilibrium cohesive energy of bulk Cu, Ag, and Au, and the same quantity computed with the PBE functional, is listed; the results are compared with the estimates reported by Rehr and Zaremba.³ Note that the “dipole-dipole contribution to the polarization force” of ref. 3 should be directly comparable with, for instance, the E_{vdW} quantity computed by our DFT/vdW-WF2p method, since it is analogous to the usual expression for the vdW interaction between atoms in a molecular crystals:⁴ particularly for Ag and Au the agreement is rather good. In line with ref. 3, if the conduction-electron screening is neglected, the vdW contributions are 2-3 times larger than the screened ones; the same is true for the semiempirical PBE-D scheme which clearly overestimates the cohesive energy, particularly for Au (see Tables II and VI). Note that reduction factors similar to ours, are suggested in ref. 24 to correct effective C_6 coefficients in noble metals, by including screening effects estimated by the Lifshitz-Zaremba-Kohn theory.⁵³

Interestingly, the RPAp method allows for a direct estimate of many-body contributions⁵⁴ to the cohesive energy in bulk noble metals. In fact, by performing a Taylor series expansion of eq.(10), truncated to second order, one obtains the following expression:

$$E_{\text{RPAp}}^{(2)} = -\frac{1}{4\pi} \int_0^\infty du \text{Tr}[(AT)^2], \quad (12)$$

which mathematically corresponds³⁹ to the pairwise summation of two-body energy contri-

butions. The quantity $E_{\text{RPAp}}^{\text{MB}} = E_{\text{RPAp}} - E_{\text{RPAp}}^{(2)}$ hence includes all many-body effects, *i.e.* all the energy contributions beyond the two-body component. By evaluating $E_{\text{RPAp}}^{\text{MB}}$ we find that many-body effects induce a significant reduction of the vdW cohesive energy and smaller changes in the other quantities: for instance, in the case of Ag, fitting the cohesive-energy curve obtained using (12) gives for the vdW contribution 0.446 eV/atom, for the equilibrium lattice constant 4.087 Å, and for the bulk modulus 1079 kbar, so that (compare with RPAp1 data in Tables III, IV, and VI) many-body effects lead to variations in these quantities by -5.2%, +0.2%, and -1.2%, respectively (once again the equilibrium lattice constant appears to be the least affected quantity). We also observe, comparing RPAp1 to RPAp2, that the first methodology, where the Hamiltonian of Eq. (8) is parameterized in such a way to reproduce the effective *screened* interatomic C_6 coefficients of ref. 4, is slightly more accurate than the second, where the C_6 coefficients turn out to be slightly underestimated. In any case this further supports the validity of the present approach, since different parameterizations lead to limited differences on the overall performances of the methods, that are in both cases similar to those obtained by DFT/vdW-WF2p.

Coming back to the good performances of the PBEsol DFT functional reported above, which are only slightly worse than those of the vdW-corrected DFT/vdW-WF2p, RPAp, and vdW-DF-cx methods, the improvement of PBEsol with respect to PBE can be explained by the fact that PBEsol restores³⁵ the density-gradient expansion appropriate for slowly varying densities (as those characterizing the valence-electron densities in densely packed solids), while PBE instead is optimized to reproduce the exchange energy of free atoms. Therefore, in PBEsol the revised exchange contribution turns out to be almost equivalent to the nonlocal vdW contribution which is added to PBE in the DFT/vdW-WF2p approach (or included in the nonlocal vdW-DF-cx functional).

As can be seen from Tables III, IV, and V, the meta-GGA TPSS functional³² performs quite well (in agreement with ref. 48) for estimating the equilibrium lattice constant and bulk modulus, however a full assessment of the method cannot be given, since, due to numerical problems in the spin-polarized calculations for the isolated atoms, the cohesive-energy estimate is not available (the same is true also in ref. 48).

Finally, data obtained³⁸ at the PBE0 level, namely using an hybrid functional which contains a certain amount of exact exchange and is much more computationally expensive than the other considered methods, are listed in Tables II, III, and IV for Cu and Ag. The

evident underestimate of the cohesive energies (14% and 22% for Cu, and Ag, respectively) and of the bulk modulus values together with the significant overestimate of the equilibrium lattice constant, clearly show that hybrid functionals such as PBE0 (or the almost equivalent HSE03 which allows to evaluate the short-range Fock operator on a coarser k mesh than PBE0³⁸) do not include vdW effects properly, as already pointed out elsewhere.⁴⁷

IV. CONCLUSIONS

In conclusion, we have computed the cohesive energy, equilibrium lattice constant, and bulk modulus of noble metals by different van der Waals-corrected Density Functional Theory methods, including vdW-DF, vdW-DF2, vdW-DF-cx, rVV10 and PBE-D. In addition, an extension of the DFT/vdW-WF2 (DFT/vdW-WF2p) scheme, based on the generation of Maximally Localized Wannier Functions, and an effective atom-based RPA (RPAp) approach (in two variants) have been specifically designed to treat the complex dynamical screening induced by delocalized s electrons. Comparison with results obtained without explicit inclusion of van der Waals effects, such as with the LDA, PBE, PBEsol, or the hybrid PBE0 methods, elucidates the importance of a suitable description of screened van der Waals effects interactions even in the case of strong metal bonding. This is particularly true for cohesive energy and bulk modulus, while lattice constants are typically already well reproduced at the LDA/GGA level. We confirm that the GGA PBEsol functional significantly improves on PBE. On the whole, the vdW-DF-cx, RPAp1, and DFT/vdW-WF2p methods give the best results. In particular, the good performances of the DFT/vdW-WF2p and RPAp schemes give further support to the simple plasma-frequency model, proposed by Maggs and Ashcroft⁴ for describing the screened vdW interactions in a polarizable metal. In fact, while conventional pairwise vdW methods show a clear tendency to overestimate cohesion, the dynamical screening acts by effectively reducing the vdW interaction, consistently improving the overall accuracy. As estimated via the RPAp method, many body effects beyond the two-body contributions induce a further reduction of the overall vdW cohesion. Due to the interplay between different energetic and screening contributions, the cohesion of noble metals hence emerges as a challenging problem, whose accurate modeling demands

the introduction of appropriate vdW-corrected DFT approaches.

- ¹ W. Liu, J. Carrasco, B. Santra, A. Michaelides, M. Scheffler, A. Tkatchenko, Phys. Rev. B **86**, 245405 (2012).
- ² K. Berland, V. R. Cooper, K. Lee, E. Schröder, T. Thonhauser, P. Hyldgaard, B. I. Lundqvist, Rep. Prog. Phys. **78**, 066501 (2015).
- ³ J. J. Rehr, E. Zaremba, W. Kohn, Phys. Rev. B **12**, 2062 (1975).
- ⁴ A. C. Maggs, N.W. Ashcroft, Phys. Rev. Lett. **59**, 113 (1987).
- ⁵ K. E. Riley, M. Pitoňák, P. Jurečka, P. Hobza, Chem. Rev. **110**, 5023 (2010).
- ⁶ A. Tkatchenko, L. Romaner, O. T. Hofmann, E. Zojer, C. Ambrosch-Draxl, and M. Scheffler, MRS Bulletin, **35**, 435 (2010).
- ⁷ J. Klimeš, A. Michaelides, J. Chem. Phys. **137**, 120901 (2012).
- ⁸ N. Marzari and D. Vanderbilt, Phys. Rev. B **56**, 12847 (1997).
- ⁹ P. L. Silvestrelli, Phys. Rev. Lett **100**, 053002 (2008).
- ¹⁰ P. L. Silvestrelli, J. Phys. Chem. A **113**, 5224 (2009).
- ¹¹ P. L. Silvestrelli, K. Benyahia, S. Grubisić, F. Ancilotto, F. Toigo, J. Chem. Phys. **130**, 074702 (2009).
- ¹² P. L. Silvestrelli, Chem. Phys. Lett. **475**, 285 (2009).
- ¹³ P. L. Silvestrelli, F. Toigo, F. Ancilotto, J. Phys. Chem. C **113**, 17124 (2009).
- ¹⁴ A. Ambrosetti, P. L. Silvestrelli, J. Phys. Chem. C **115**, 3695 (2011).
- ¹⁵ F. Costanzo, P. L. Silvestrelli, Francesco Ancilotto, J. Chem. Theory Comp. **8**, 1288 (2012); Archives of Metallurgy and Materials **57**, 1075 (2012).
- ¹⁶ P. L. Silvestrelli, A. Ambrosetti, S. Grubisić, and F. Ancilotto, Phys. Rev. B **85**, 165405 (2012).
- ¹⁷ A. Ambrosetti, F. Ancilotto, P. L. Silvestrelli, J. Phys. Chem. C **117**, 321 (2013).
- ¹⁸ A. Ambrosetti, P. L. Silvestrelli, Phys. Rev. B **85**, 073101 (2012).
- ¹⁹ P. L. Silvestrelli and A. Ambrosetti, Phys. Rev. B **87**, 075401 (2013).
- ²⁰ P. L. Silvestrelli, J. Chem. Phys. **139**, 054106 (2013).
- ²¹ P. L. Silvestrelli, A. Ambrosetti, J. Chem. Phys. **140**, 124107 (2014).
- ²² P. L. Silvestrelli, A. Ambrosetti, Phys. Rev. B **91**, 195405 (2015).
- ²³ W. L. Bade, J. Chem. Phys. **27**, 1280 (1957).

- ²⁴ V. G. Ruiz, W. Liu, E. Zojer, M. Scheffler, A. Tkatchenko, Phys. Rev. Lett. **108**, 146103 (2012); W. Liu, A. Tkatchenko, and M. Scheffler, Acc. Chem. Res. **47**, 3369 (2014).
- ²⁵ S. Grimme, J. Comp. Chem. **27**, 1787 (2006); V. Barone, M. Casarin, D. Forrer, M. Pavone, M. Sambi, A. Vittadini, J. Comp. Chem. **30**, 934 (2009).
- ²⁶ M. Dion, H. Rydberg, E. Schröder, D. C. Langreth, B. I. Lundqvist, Phys. Rev. Lett. **92**, 246401 (2004); G. Roman-Perez, J. M. Soler, Phys. Rev. Lett. **103**, 096102 (2009).
- ²⁷ T. Thonhauser, V. R. Cooper, S. Li, A. Puzder, P. Hyldgaard, D. C. Langreth, Phys. Rev. B **76**, 125112 (2007).
- ²⁸ K. Lee, É. D. Murray, L. Kong, B. I. Lundqvist, and D. C. Langreth, Phys. Rev. B **82**, 081101(R) (2010).
- ²⁹ K. Berland, P. Hyldgaard, Phys. Rev. B **89**, 035412 (2014).
- ³⁰ K. Berland, Calvin A. Arter, Valentino R. Cooper, Kyuho Lee, Bengt I. Lundqvist, Elsebeth Schröder, T. Thonhauser, and Per Hyldgaard, J. Chem. Phys. **140**, 18A539 (2014).
- ³¹ R. Sabatini, T. Gorni, S. de Gironcoli, Phys. Rev. B **87**, 041108(R) (2013).
- ³² J. Tao, J. P. Perdew, V. N. Staroverov, and G. E. Scuseria, Phys. Rev. Lett. **91**, 146401 (2003).
- ³³ C. Adamo, V. Barone, J. Chem. Phys. **110**, 6158 (1999).
- ³⁴ J. P. Perdew, K. Burke, M. Ernzerhof, Phys. Rev. Lett. **77**, 3865 (1996).
- ³⁵ John P. Perdew, Adrienn Ruzsinszky, Gabor I. Csonka, Oleg A. Vydrov, Gustavo E. Scuseria, Lucian A. Constantin, Xiaolan Zhou, and Kieron Burke, Phys. Rev. Lett. **100**, 136406 (2008).
- ³⁶ O. A. Vydrov, T. Van Voorhis, J. Chem. Phys. **133**, 244103 (2010).
- ³⁷ P. Haas, F. Tran, P. Blaha, Phys. Rev. B **79**, 085104 (2009).
- ³⁸ J. Heyd, G. E. Scuseria, M. Ernzerhof, J. Chem. Phys. **118**, 8207 (2003); J. Paier, M. Marsman, K. Hummer, G. Kresse, I. C. Gerber, J. G. Angyan, J. Chem. Phys. **124**, 154709 (2006).
- ³⁹ A. Tkatchenko, A. Ambrosetti, R.A. DiStasio Jr., J. Chem. Phys. **138**, 074106 (2013).
- ⁴⁰ A. Ambrosetti, A.M. Reilly, R.A. DiStasio Jr., A. Tkatchenko J. Chem. Phys. **140**, 18A508 (2014).
- ⁴¹ R. Eisenhitz, F. London, Z. Phys. **60**, 491 (1930).
- ⁴² T. Brink, J. S. Murray, P. Politzer, J. Chem. Phys. **98**, 4305 (1993).
- ⁴³ A. Tkatchenko, M. Scheffler, Phys. Rev. Lett. **102**, 073005 (2009).
- ⁴⁴ S. Grimme, J. Antony, T. Schwabe, C. Mück-Lichtenfeld, Org. Biomol. Chem. **5**, 741 (2007); S. Grimme, J. Antony, S. Ehrlich, H. Krieg, J. Chem. Phys. **132**, 154104 (2010).

- ⁴⁵ P. Giannozzi, S. Baroni, N. Bonini, M. Calandra, R. Car, C. Cavazzoni, D. Ceresoli, G. L. Chiarotti, M. Cococcioni, I. Dabo, A. Dal Corso, S. Fabris, G. Fratesi, S. de Gironcoli, R. Gebauer, U. Gerstmann, C. Gougoussis, A. Kokalj, M. Lazzeri, L. Martin-Samos, N. Marzari, F. Mauri, R. Mazzarello, S. Paolini, A. Pasquarello, L. Paulatto, C. Sbraccia, S. Scandolo, G. Sclauzero, A. P. Seitsonen, A. Smogunov, P. Umari, R. M. Wentzcovitch, *J.Phys.: Condens. Matter* **21**, 395502 (2009), <http://arxiv.org/abs/0906.2569>.
- ⁴⁶ WanT code by A. Ferretti, B. Bonferroni, A. Calzolari, and M. Buongiorno Nardelli, <http://www.wannier-transport.org> ; see also A. Calzolari, N. Marzari, I. Souza and M. Buongiorno Nardelli, *Phys. Rev. B* **69**, 035108 (2004).
- ⁴⁷ W. Liu, V. G. Ruiz, G.-X. Zhang, B. Santra, X. Ren, M. Scheffler, A. Tkatchenko, *New J. Phys.* **15**, 053046 (2013); V. G. Ruiz, W. Liu, A. Tkatchenko, *Phys. Rev. B* **93**, 035118 (2016).
- ⁴⁸ Gabor I. Csonka, John P. Perdew, Adrienn Ruzsinszky, Pier H. T. Philipsen, Sebastien Lebegue, Joachim Paier, Oleg A. Vydrov, and Janos G. Angyan, *Phys. Rev. B* **79**, 155107 (2009).
- ⁴⁹ See, for instance: N. W. Ashcroft and N. D. Mermin, *Solid State Physics*, Holt-Saunders International Editions, Philadelphia, 1976.
- ⁵⁰ F. D. Murnaghan, *Proc. Natl. Acad. Sci. U.S.A.* **30**, 244 (1944).
- ⁵¹ Marta Rosa, Stefano Corni, and Rosa Di Felice, *Phys. Rev. B* **90**, 125448 (2014).
- ⁵² I. Souza, N. Marzari, D. Vanderbilt, *Phys. Rev. B* **65**, 035109 (2001).
- ⁵³ E. M. Lifshitz, *Soviet Physics JETP* **2**, 73 (1956); E. Zaremba and W. Kohn, *Phys. Rev. B* **13**, 2270 (1976).
- ⁵⁴ A. Ambrosetti, D. Alfè , R.A. DiStasio Jr., A. Tkatchenko, *J. Phys. Chem. Lett.* **5**, 849 (2014).

TABLE I: Fitted static polarizabilities and oscillator frequencies (in a.u.) adopted in the RPAp1 and RPAp2 methods (see text).

method	Cu	Ag	Au
α_0	11.7	14.6	19.5
ω_0 RPAp1	0.58	0.84	0.80
ω_0 RPAp2	0.46	0.75	0.68

TABLE II: Equilibrium cohesive energy E_c (in eV/atom) of bulk Cu, Ag, and Au, using different methods. Results are compared with available experimental reference data corrected by finite-temperature and zero-point effects (see text).

method	Cu	Ag	Au
LDA	4.353	3.612	4.357
PBE	3.323	2.513	3.042
PBEsol	3.895	3.088	3.682
PBE-D	3.721	3.078	4.456
rVV10	3.392	2.835	3.533
vdW-DF	2.732	2.189	2.694
vdW-DF2	2.574	2.038	2.515
vdW-DF-cx	3.636	3.075	3.754
PBE0 ^a	3.046	2.329	—
DFT/vdW-WF2	4.589	3.469	4.874
DFT/vdW-WF2p	3.697	2.808	3.523
RPAp1	3.636	2.937	3.586
RPAp2	3.569	2.879	3.466
expt.	3.524	2.972	3.810

^aref.38.

TABLE III: Equilibrium lattice constant a_0 (in Å) of bulk Cu, Ag, and Au, using different methods. Results are compared with available experimental reference data corrected by finite-temperature and zero-point effects (see text).

method	Cu	Ag	Au
LDA	3.553	4.020	4.053
PBE	3.676	4.163	4.173
PBEsol	3.585	4.063	4.099
PBE-D	3.615	4.155	4.026
rVV10	3.699	4.219	4.211
vdW-DF	3.754	4.262	4.249
vdW-DF2	3.788	4.276	4.286
vdW-DF-cx	3.627	4.103	4.108
TPSS	3.607	4.136	4.127
PBE0 ^a	3.636	4.142	—
DFT/vdW-WF2	3.599	3.975	3.996
DFT/vdW-WF2p	3.641	4.088	4.108
RPAp1	3.646	4.094	4.113
RPAp2	3.658	4.106	4.128
expt.	3.595	4.056	4.062

^aref.38.

TABLE IV: Equilibrium bulk modulus B (in kbar) of bulk Cu, Ag, and Au, using different methods. Results are compared with available experimental reference data corrected by finite-temperature and zero-point effects (see text).

method	Cu	Ag	Au
LDA	1715	1386	1945
PBE	1286	912	1430
PBEsol	1662	1196	1739
PBE-D	1332	650	1825
rVV10	1229	867	1377
vdW-DF	1042	799	1206
vdW-DF2	1080	1434	1746
vdW-DF-cx	1495	1105	1701
TPSS	1688	1040	1698
PBE0 ^a	1300	868	—
DFT/vdW-WF2	2646	1473	2843
DFT/vdW-WF2p	1581	1071	1727
RPAp1	1511	1067	1649
RPAp2	1433	1035	1570
expt.	1420	1090	1965

^aref.38.

TABLE V: Mean relative error (MRE) and, in parenthesis, mean absolute relative error (MARE) relative to cohesive energy, lattice constant and bulk modulus, and, in square parenthesis, MARE value averaged on the 3 different quantities considered (AMARE), using different methods, listed in order of decreasing performance (increasing AMARE value).

method	E_c	a_0	B	AMARE
vdW-DF-cx	-0.5 (2.7)	1.1 (1.1)	-2.3 (6.7)	[3.5]
RPAp1	-1.3 (3.4)	1.2 (1.2)	-3.9 (8.2)	[4.3]
DFT/vdW-WF2p	-2.7 (6.0)	1.1 (1.1)	0.5 (7.1)	[4.7]
RPAp2	-3.6 (4.5)	1.5 (1.5)	-8.1 (8.7)	[4.9]
PBEsol	3.6 (5.9)	0.2 (0.5)	5.1(12.8)	[6.4]
PBE-D	8.8 (8.8)	0.6 (1.2)	-17.9(17.9)	[9.3]
rVV10	-6.8 (6.8)	3.5 (3.5)	-21.3(21.3)	[10.5]
PBE	-13.8(13.8)	2.5 (2.5)	-17.7(17.7)	[11.3]
LDA	19.8(19.8)	-0.8 (0.8)	15.6(16.3)	[12.3]
vdW-DF2	-31.2(31.2)	5.5 (5.5)	-1.2(22.2)	[19.6]
vdW-DF	-27.1(27.1)	4.7 (4.7)	-30.6(30.6)	[20.8]
DFT/vdW-WF2	24.9(24.9)	-1.2 (1.3)	55.4(55.4)	[27.2]
TPSS	—	1.4 (1.4)	0.2(12.3)	—

TABLE VI: vdW contribution, E_{vdW} , in eV/atom, (in percentage with respect to the total cohesive energy in parenthesis), defined as the difference between the equilibrium cohesive energy of bulk Cu, Ag, and Au, and the same quantity computed with the PBE functional. Results are compared with the estimates by Rehr and Zaremba³ (in square parenthesis the dipole-dipole contribution to the polarization force which is analogous to the usual expression for the vdW interaction between atoms in a molecular crystal⁴).

method	Cu	Ag	Au
PBE-D	0.398 (11%)	0.565 (18%)	1.414 (32%)
DFT/vdW-WF2	1.123 (25%)	0.809 (24%)	1.731 (36%)
DFT/vdW-WF2p	0.374 (10%)	0.295 (11%)	0.481 (14%)
RPAp1	0.313 (9%)	0.424 (14%)	0.544 (15%)
RPAp2	0.246 (7%)	0.366 (13%)	0.424 (12%)
ref. 3	0.21 (6%)	0.42 (14%)	0.63 (17%)
ref. 3	[0.179 (5%)]	[0.347 (12%)]	[0.524 (14%)]

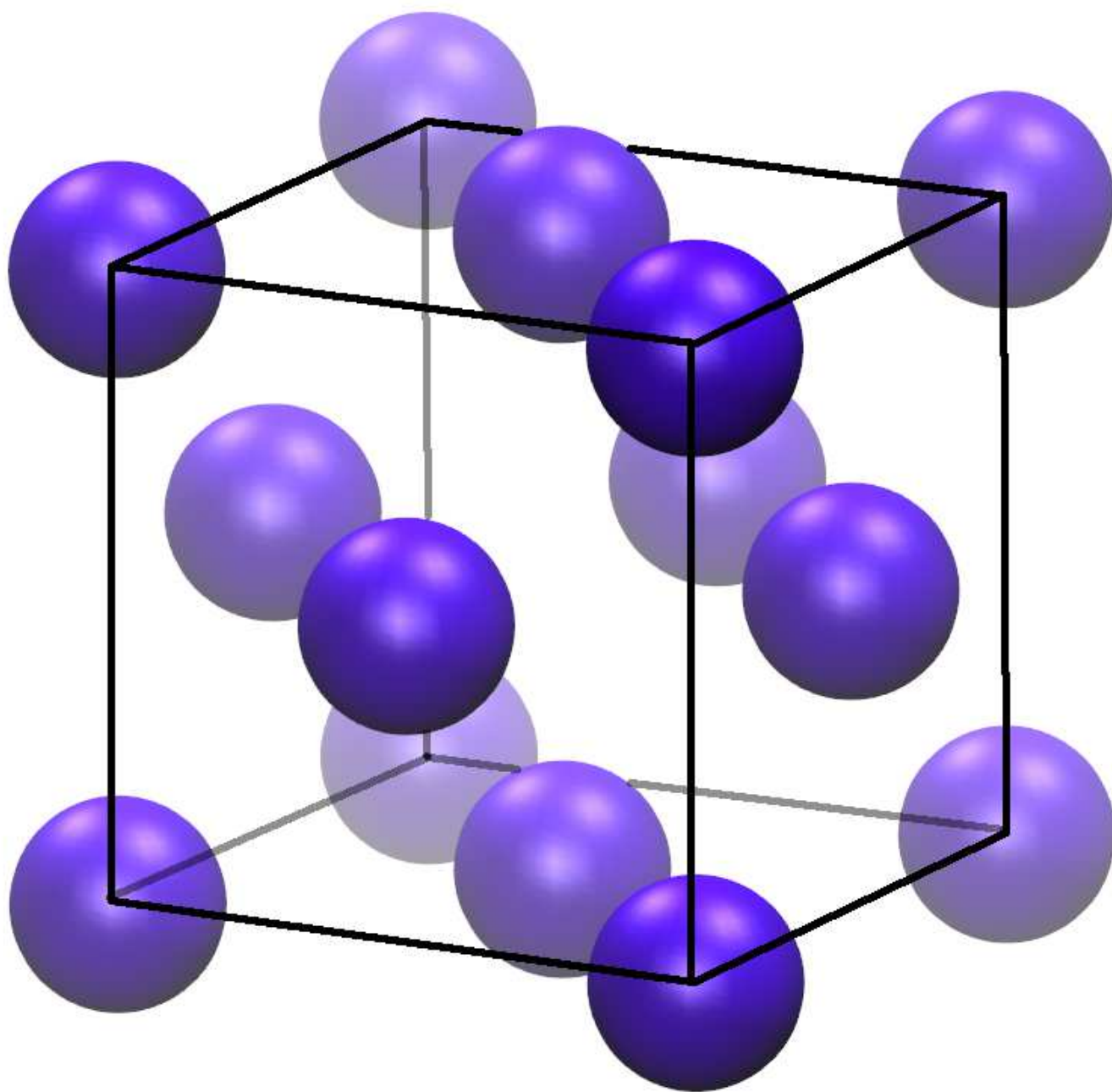
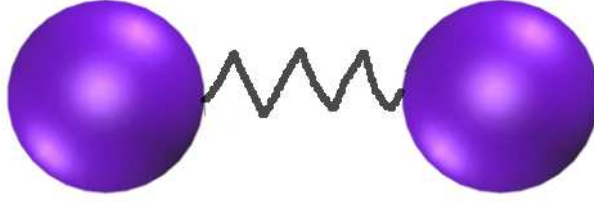


FIG. 1: Equilibrium crystal structure, face-centered-cubic (FCC), of Cu, Ag, and Au.

a)



b)

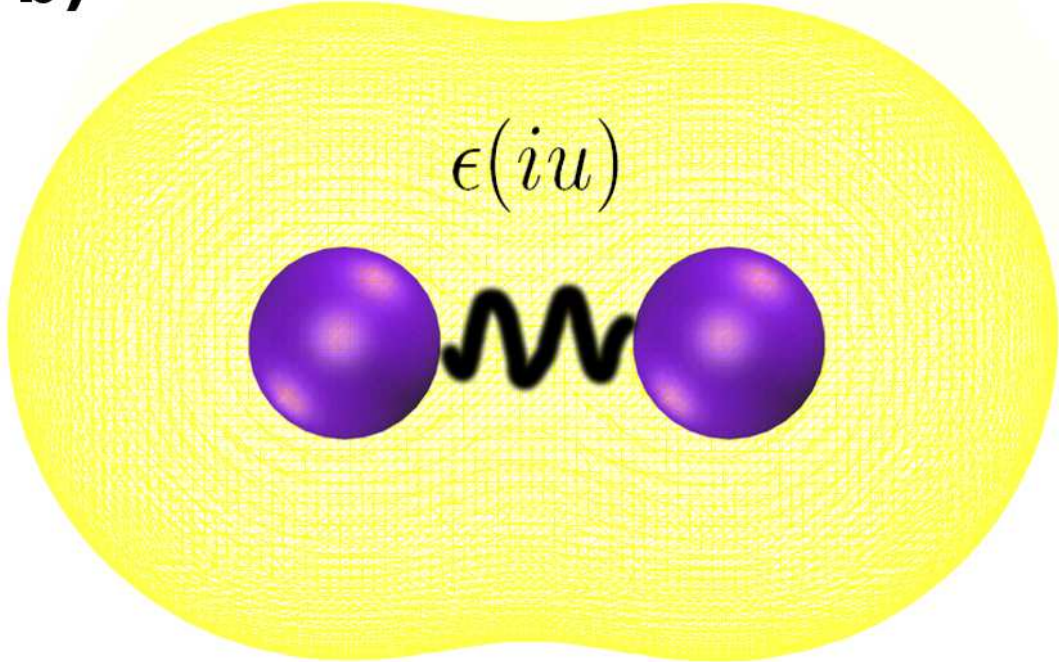


FIG. 2: Intuitive representation of screened vdW interactions in noble metals. In panel **a)** two atoms interact via unscreened dipole-dipole interaction, as in molecular crystals. In panel **b)** the presence of a medium made of delocalized electrons introduces in noble metals a dynamical screening of the dipole-dipole interaction, effectively described by the dielectric function $\epsilon(iu)$.

